Developmental Cell, Vol. 9, 283–292, August, 2005, Copyright ©2005 by Elsevier Inc. DOI 10.1016/j.devcel.2005.05.016

Wnt9b Plays a Central Role in the Regulation of Mesenchymal to Epithelial Transitions Underlying Organogenesis of the Mammalian Urogenital System

Thomas J. Carroll,[1] Joo-Seop Park, Shigemi Hayashi,[2] Arindam Majumdar,[3] and Andrew P. McMahon*
Department of Molecular and Cellular Biology
Harvard University
16 Divinity Avenue
Cambridge, Massachusetts 02138

Summary

The vertebrate urogenital system forms due to inductive interactions between the Wolffian duct, its derivative the ureteric bud, and their adjacent mesenchymes. These establish epithelial primordia within the mesonephric (embryonic) and metanephric (adult) kidneys and the Müllerian duct, the anlage of much of the female reproductive tract. We show that *Wnt9b* is expressed in the inductive epithelia and is essential for the development of mesonephric and metanephric tubules and caudal extension of the Müllerian duct. *Wnt9b* is required for the earliest inductive response in metanephric mesenchyme. Further, *Wnt9b*-expressing cells can functionally substitute for the ureteric bud in these interactions. Wnt9b acts upstream of another Wnt, Wnt4, in this process, and our data implicate canonical Wnt signaling as one of the major pathways in the organization of the mammalian urogenital system. Together these findings suggest that Wnt9b is a common organizing signal regulating diverse components of the mammalian urogenital system.

Introduction

The mammalian urogenital system (UGS) develops from a region of mesoderm that lies ventral to the somites and dorsal to the lateral plate known as the intermediate mesoderm (IM). At mouse embryonic day 9.5 (E9.5), the UGS consists of a pair of epithelial ducts (the Wolffian ducts) that run ventral to the somites, extending from the level of the forelimb to the cloaca. A signal(s) emanating from the duct induces a mesenchymal to epithelial transition (MET) within a medial population of the IM leading to the formation of the mesonephric tubules (Boyden, 1927; Gruenwald, 1937; Sainio, 2003a; Waddington, 1938). The mesonephric tubules and the Wolffian duct together form the mesonephric kidney, a transient nonessential embryonic organ in the mouse. By E10.5, the Wolffian duct forms a dorsal branch, the ureteric bud (UB), that enters a population of prespecified IM at the hindlimb level known as the metanephric mesenchyme (MM). All subsequent development of the metanephric kidney, the functional kidney throughout postnatal life, is dependent on interactions between the UB and MM. The UB derivatives give rise to the highly branched collecting duct network of the mature organ (Saxen, 1987). The remaining nonvascular components of the kidney arise from MM progenitors that cap the tips of the branching UB. Here, a signal(s) from the ureteric bud induces MM to undergo a MET leading to formation of epithelial renal vesicles (RV), precursors of the main epithelial body of the nephron, the functional unit of the metanephric kidney (Mori et al., 2003).

In addition to its central role in the induction of mesonephric and metanephric kidneys, the Wolffian duct is also critical for development of the reproductive system (Kobayashi and Behringer, 2003). While the Wolffian duct itself forms the vas deferens and seminiferous tubules of the male reproductive system, the epididymis is derived from the mesonephric tubules. In females, the oviducts, uterus, and upper vagina derive from the Müllerian duct, and normal development of this duct requires Wolffian duct signaling (Gruenwald, 1942). In summary, the Wolffian duct and its UB derivative play a central role in organizing development of many epithelial structures that are critical to urogenital function.

The molecular nature of each of these interactions is currently unclear. For example, whereas several factors have been implicated in induction of the RV (for review, see Carroll and McMahon, 2003; Mori et al., 2003), including leukemia inhibitory factor (LIF) (Barasch et al., 1999; Plisov et al., 2001) and members of the Wnt family (Herzlinger et al., 1994; Kispert et al., 1998), only one of these, *Wnt4*, is both necessary (based on *Wnt4* mutant analysis) and sufficient (based on cell-induction assays in vitro) for RV induction in the mouse (Kispert et al., 1998; Stark et al., 1994). However, *Wnt4* is expressed within the MM and is most likely itself a response to UB signaling lying downstream of the primary inductive factor(s) (Stark et al., 1994). Here, we identify *Wnt9b* as a Wnt family member that is expressed within the Wolffian duct and its derivative. Genetic and cell culture assays demonstrate that *Wnt9b* signaling plays a primary role in induction of the mammalian kidney and reproductive system.

Results

Wnt9b Expression in the Wolffian Duct and Its Derivatives

Wnt9b (previously known as *Wnt14b* [Qian et al., 2003; Kirikoshi et al., 2001] and *Wnt15* [Bergstein et al., 1997]) is expressed throughout the Wolffian duct epithelium in both sexes from E9.5 (Figure 1A) to E14.5 (data not shown). In the metanephric kidney, *Wnt9b* is expressed in the ureteric bud as it invades the metanephric anlage at E10.5–E11.0 (Figure 1B). Unlike *Wnt11*, which is expressed at the tip of the ureteric bud (Figure 1C), *Wnt9b* is downregulated in this region and expressed more

*Correspondence: mcmahon@mcb.harvard.edu
[1]Present address: Department of Internal Medicine, University of Texas Southwestern Medical School, 5323 Harry Hines Boulevard, Dallas, Texas 75390.
[2]Present address: Novartis Institute for Biomedical Research, 250 Massachusetts Avenue, Cambridge, Massachusetts 02139.
[3]Present address: Department of Medical Biochemistry and Biophysics, Division of Matrix Biology, Karolinska Institutet, Scheeles väg 2 SE-171 77 Stockholm, Sweden.

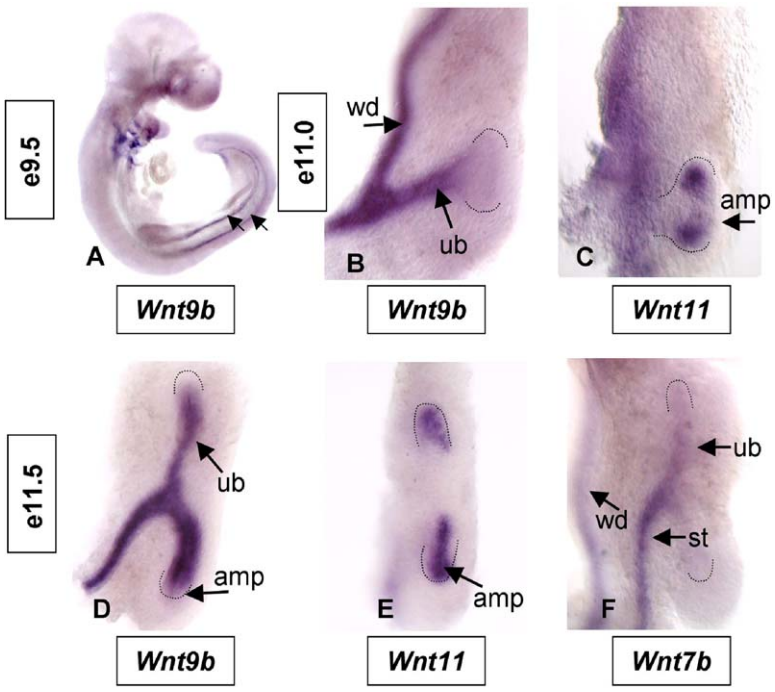

Figure 1. Urogenital Expression of *Wnt7b, Wnt9b*, and *Wnt11*

Wolffian duct and ureteric bud expression of *Wnt9b* (A, B, and D), *Wnt11* (C and E), and *Wnt7b* (F) in the E9.5 (A), E11.0 (B and C), and E11.5 (D–F) mouse embryos. Embryos in (B)–(F) are littermates. Arrows in (A) indicate paired Wolffian ducts. See text for details. amp, ureteric bud ampullae; st, ureteric bud stalk; ub, ureteric bud; wd, Wolffian duct.

strongly in the stalk. At E11.5, the bud has undergone the first of a series of iterative branching events to generate the T-stage. At this time, *Wnt9b* expression is high in the stalk and horizontal epithelium of the T but is downregulated in the proximal branching tips where *Wnt11* is highly expressed (compare Figures 1D and 1E). Expression of *Wnt9b* in the ventral epithelium precedes and correlates with the appearance of the first RV's adjacent to this epithelium (see later). A third Wnt, *Wnt7b*, is coexpressed, albeit weakly, with *9b* in the Wolffian duct and stalk of the UB, but its expression does not extend into proximal branching epithelium (Figure 1F). *Wnt9b* continues to be expressed in the developing collecting duct system throughout nephrogenesis where expression extends into the branching epithelium but not to the branching tips (not shown). At E15.5, expression is confined to the kidney; the extrarenal ureter, which expresses Wnt7b, does not express *Wnt9b* (not shown).

Wnt9b Is Essential for Metanephric Kidney Development

To address the role of *Wnt9b* in nephrogenesis, we generated a likely conditional null allele, $Wnt9b^{c}$. A second allele where lox-p sites flank exon 2, $Wnt9b^{cneo}$, represents an intermediate stage prior to Flp-mediated excision of a PGK-neomycin selection cassette in the second intron (see Supplemental Figure S1 available with this article online). Cre-mediated excision of exon 2 is predicted to result in out-of-frame splicing of exon 1 to exon 3, and consequently a mutant transcript that would encode a nonfunctional peptide comprising the first 27 amino acids of Wnt9b that comprises the signal peptide. This putative null allele we refer to as $Wnt9b^{-}$.

Embryos homozygous for the $Wnt9b^{-}$ allele develop to term but die within 24 hr of birth. In addition to displaying incompletely penetrant cleft lip and palate, phenotypes that correlate with the other major site of *Wnt9b* expression in the developing face (to be described elsewhere), pups homozygous for the null allele possess only vestigial kidneys (compare Figures 2A and 2B with Figures 2E and 2F). The ureter, a derivative of the unbranched ureteric bud, connects the rudimentary kidneys to the bladder. Histological analysis reveals a population of peripheral mesenchyme (arrowhead in Figure 2L) and some rudimentary epithelia (arrow in Figure 2L) that are positively labeled by the dolichos biflorus lectin (not shown), a ureteric epithelium marker, but no nephrons or intermediate precursor stages. $Wnt9b^{cneo/-}$ and $Wnt9b^{cneo/cneo}$ pups that retain PGKneo in the active *Wnt9b* locus show an intermediate phenotype, small kidneys with few mature nephrons (Figures 2C and 2D and data not shown), that would suggest partial loss-of-function and a dose-dependent requirement for Wnt9b during kidney morphogenesis.

Further analysis indicated that $Wnt9b^{-/-}$ mutants also lack the reproductive ducts at birth: the epididymis and vas deferens in males and most of the oviduct, the uterus, and upper vagina of females (Figures 2G–2J and data not shown); in contrast, gonad development appeared largely normal. Thus, Wnt9b is required for multiple aspects of urogenital development.

Wnt9b Mutant Mesenchyme Fails to Aggregate and Undergo Tubulogenesis

To determine the molecular basis for the *Wnt9b* action, we focused on the best understood of these inductive events: RV induction in the metanephric kidney. Prior to ureteric bud invasion at E10.5, the metanephros expresses a number of molecular markers including *Pax2,*

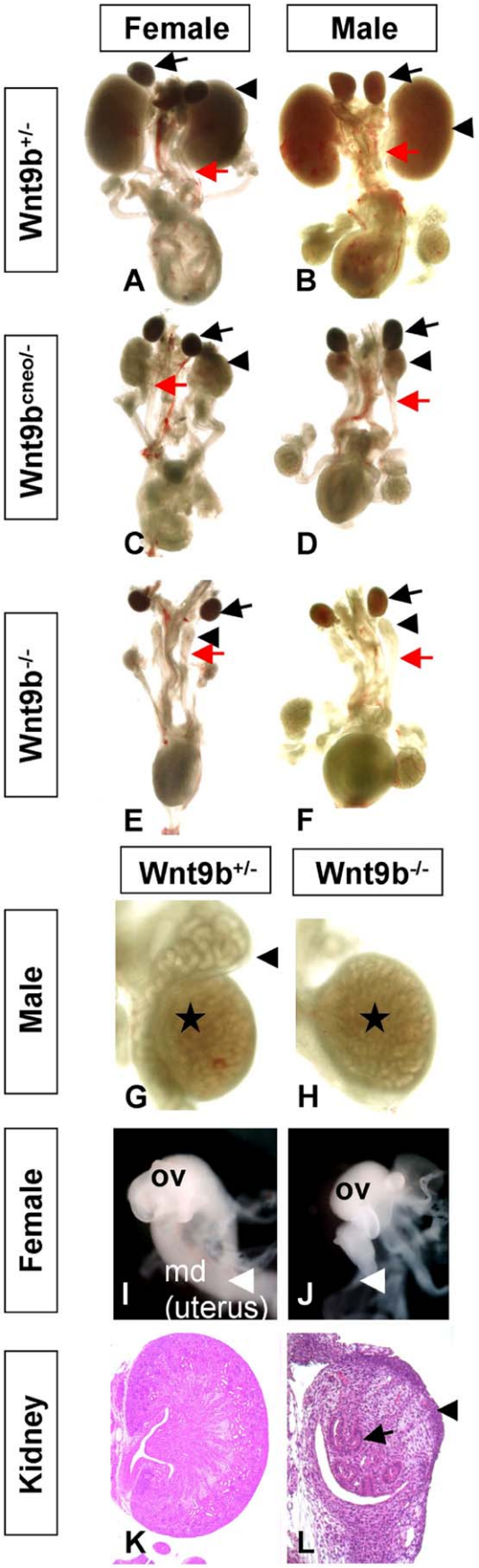

Eya1, Wt1, and *Six2* (Donovan et al., 1999; Kalatzis et al., 1998). Expression of these genes continues after ureteric bud invasion in condensed MM that caps the branching ureteric bud throughout the period of kidney organogenesis. The condensed mesenchyme also expresses several additional genes in association with UB bud invasion including *integrinα8* and *Bmp7*, the former being essential for maintenance of the condensate (Godin et al., 1998; Muller et al., 1997). The first cellular evidence of MM induction is the formation of pretubular cellular aggregates at E11.75–E12.00 and epithelial RVs at E12.5 (Bard et al., 2001).

In *Wnt9b*$^{-/-}$ embryos, ureteric bud invasion of the metanephric mesenchyme occurs at the appropriate stage and the first branching event is initiated (Figures 3A and 3B and not shown). The condensed mesenchyme expresses *Pax2, Eya1, Wt1, Bmp7, integrinα8*, and *Six2* as expected, although by E12.5 their expression domains are reduced compared to wild-type (Figures 3C and 3D and not shown). Thus, Wnt9b is not essential for early development of the ureteric component of the metanephric kidney, or for either formation or initial maintenance of the condensed MM progenitor population. However, subsequent branching after the T-stage is disrupted. Branching growth of the ureteric epithelium is critically dependent on mesenchymal GDNF signaling through the c-Ret/GFR1a receptor complex in the ureteric epithelium (Angrist et al., 1996; Jing et al., 1996; Moore et al., 1996; Sanchez et al., 1996; Schuchardt et al., 1994, 1996; Tomac et al., 2000; Treanor et al., 1996), an interaction maintained in part by a Wnt11-GDNF-positive regulation loop (Majumdar et al., 2003). Whereas *c-Ret* expression is unaltered in *Wnt9b*$^{-/-}$ mutants (Figures 3E and 3F), a downregulation of *Wnt11* (Figures 3G and 3H) and *GDNF* (Figures 3I and 3J) expression is observed preceding the branching defect, suggesting a later requirement for Wnt9b in the regulation of secondary branching.

We next attempted to address the issue of RV induction in *Wnt9b* mutants, focusing on the earliest responses of the MM to the UB to exclude secondary phenotypes due to defective branching. At (but not prior to) E11, diffuse weak mesenchymal expression of *Wnt4, Fgf8*, and *Pax8* was detected in MM surrounding the unbranched ureteric bud tip in wild-type and *Wnt9b*$^{+/-}$ kidneys (not shown). By E11.5, all or the ma-

Figure 2. Gross Phenotype of *Wnt9b* Mutant Urogenital System

Intact urogenital systems from E18.5 females (A, C, and E) and males (B, D, and F). In Wnt9b heterozygotes (A and B), the adrenal glands (arrows), kidneys (arrowheads), and ureters (red arrows) appear normal. In Wnt9b$^{cneo/-}$ embryos (C and D), the kidneys are greatly reduced in size. In Wnt9b$^{-/-}$ pups (E and F), the kidneys are absent although the adrenal glands and ureter appear normal. Close examination of heterozygous (G) and mutant (H) males reveals normal testis (stars) but the absence of the epididymis in mutants (arrow in [G]). Mutant females posses normal ovaries but lack a uterus (arrowhead in [J]) and upper vagina (not shown). Hematoxylin and eosin sections through heterozygous (K) and null (L) kidneys show a small population of mesenchymal cells (arrowhead in [L]) adjacent to the slightly branched collecting duct system (arrow in [L]). There is no morphological or molecular evidence of mesenchymally derived tubular epithelia in mutants.

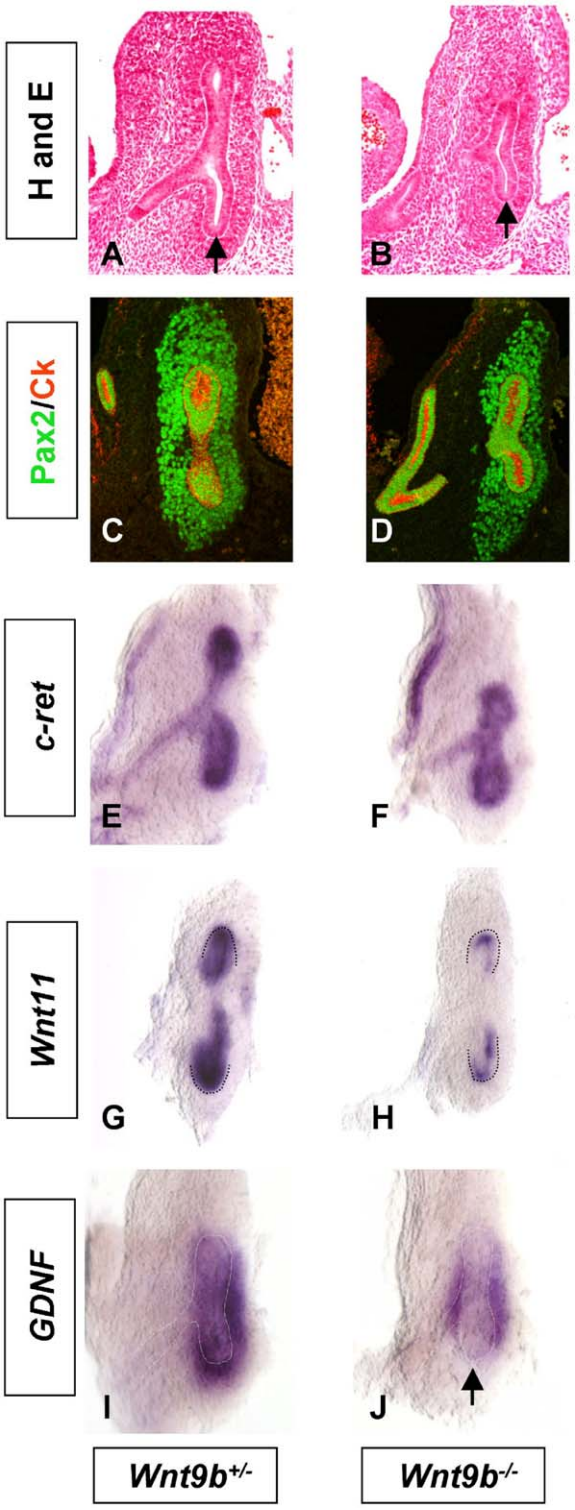

Figure 3. The Ureteric Bud Forms and the Initial Branch Is Normal in *Wnt9b*$^{-/-}$ Mutants

At E11.5, the mutant ureteric bud (B, D, F, H, and J) has branched once, forming a T-shape similar to the case in wild-type littermates (A, C, E, G, and I). Hematoxylin and eosin staining (A and B) and immunofluorescence with antibodies to Pax2 (green in [C] and [D]) and cytokeratin (red, [C] and [D]) show that the bud (arrows in [A] and [B] and cytokeratin-positive structures in [C] and [D]) has undergone the first branching event within the metanephric mesenchyme. The mutant bud expresses *cRet* transcripts at similar levels to wild-type (compare [E] and [F]). However, GDNF is expressed at lower levels when contralateral kidneys from wild-type (I) and mutant (J) kidneys are compared, most notably directly adjacent to the bud tips (arrowhead in [J]). Wnt11 expression at the bud tips is correspondingly reduced at E11.5 (compare [G] and [H]) and is completely absent by E12.0 (data not shown). Decreased GDNF/cRet signaling most likely accounts for defective secondary branching.

jority of their expression localized to the ventral half of the MM (Figures 4B–4D). By E11.75–E12.0, the tips of the ureteric bud have formed a clover-like structure just prior to each tip undergoing a trichotomous branching event (Majumdar et al., 2003). Expression of all three genes continued in the ventral MM but expression was greatly upregulated in a small subset of the ventral MM, a population that also expresses the transcriptional regulator *Lhx1* (Figures 4F–4H and data not shown). These domains mark the pretubular aggregates that prefigure tubule formation. In contrast, no mesenchymal expression of any of these genes was detected in *Wnt9b*$^{-/-}$ mutants at any stage, though *Pax8* and *Lhx1* were expressed as normal in the UB epithelium (Figures 4I–4K and data not shown). Thus, *Wnt9b* is essential for the induction of these earliest markers of the tubulogenic program.

These data indicate that Wnt9b acts upstream of Wnt4, which is itself required for RV induction at these stages (Kispert et al., 1998; Stark et al., 1994). In contrast to *Wnt9b*$^{-/-}$ mutants, *Pax8* and *FGF8* were both initially expressed at E11.5 in *Wnt4*$^{-/-}$ mutants (Figures 4L and 4M). However, by E12.5, no mesenchymal expression of either gene was detected. *Lhx1* was not detected in MM derivatives between E11.5 and E12.5 (data not shown). Together, these data suggest that initial induction of *Fgf8* and *Pax8* in response to Wnt9b signaling is Wnt4 independent, but that Wnt4 may play a critical role in maintaining and upregulating their expression in association with the formation of the pretubular aggregate. In contrast, initial *Lhx1* expression in the pretubular aggregate is dependent on Wnt4 signaling. We also observed that *GDNF* expression was maintained at normal levels in the condensed mesenchyme of later stage *Wnt4*$^{-/-}$ kidneys in contrast to *Wnt9b* mutants, an observation that correlates with the more extensive UB branching reported in the *Wnt4* mutant (Stark et al., 1994, see Discussion).

Wnt9b Is a Paracrine Signal in RV Induction

Previous studies have shown that NIH3T3 cells expressing any of several Wnt ligands can induce isolated metanephric mesenchyme to undergo tubulogenesis (Herzlinger et al., 1994; Kispert et al., 1998). In order to test whether *Wnt9b* can induce tubulogenesis, mouse NIH3T3 and L cells were stably transfected with a full-length *Wnt9b* construct and cocultured with isolated metanephric mesenchyme. As a positive control, isolated MM was cocultured with dorsal spinal cord or NIH3T3 cells expressing *Wnt1, Wnt3a*, or *Wnt4*, all of which have been shown to induce RV formation in vitro (Herzlinger et al., 1994; Kispert et al., 1998). As shown

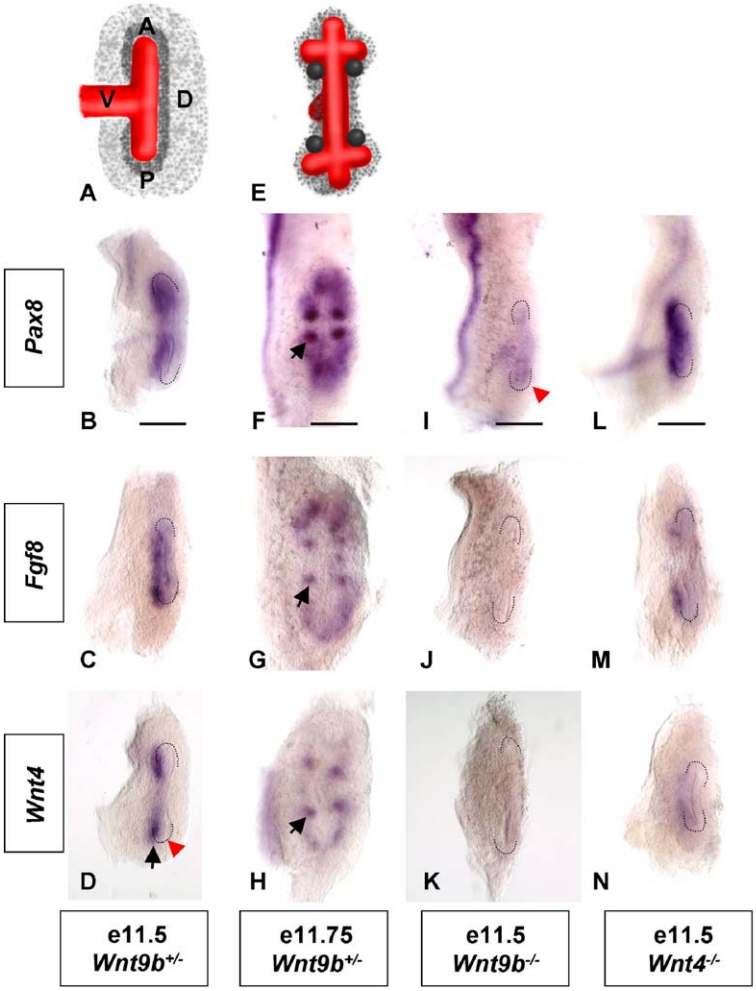

Figure 4. Dynamic Expression Patterns of "Induced Genes" within Wild-Type and Mutant Metanephric Mesenchyme

(A) and (E) show schematic representations of lateral views of E11.5 (A–D, I–N) and dorsal views of E11.75 (E–H) kidneys. Anterior is always at the top and posterior at the bottom. For lateral view, dorsal is always to the right, ventral to the left, and the ureteric bud is outlined. Kidneys were hybridized with antisense probes to *Pax8* (B, F, I, and L), *Fgf8* (C, G, J, and M), and *Wnt4* (D, H, K, and N) from wild-type (A–H), *Wnt9b* mutant (I–K), and *Wnt4* mutant (L–N) embryos. At E11.5, *Pax8*, *Fgf8*, and *Wnt4* are primarily expressed on the ventral side of the ureteric bud. Although *Pax8* shows low levels of expression in the ureteric bud (B) and in some instances a small domain of *Fgf8* can be detected in the dorsal mesenchyme (not shown), *Wnt4* seems to be expressed solely in the mesenchyme (black arrow in [D]) ventral to the ureteric bud (red arrowhead in [D]). By E11.75, all three genes are expressed at high levels within a subpopulation of mesenchyme adjacent to the branching bud. These cell clusters have no detectable lumen (not shown) and are therefore referred to as pretubular aggregates (arrows in [F]–[H]). Expression is maintained in these cells as they epithelialize, generating the renal vesicles approximately 12 hr later (data not shown). No mesenchymal expression of any of these genes is detectable in E11.5 *Wnt9b* mutants, ([I]–[K] and not shown), although expression of *Pax8* in the ureteric bud is maintained (red arrowhead in [I] and not shown). In contrast, in E11.5 *Wnt4* mutants, *Pax8* is expressed normally (L) and low levels of *Fgf8* (M) and *Wnt4* itself (N) can be detected. Mesenchymal expression of *Lhx1* is undetectable in both *Wnt9b* and *Wnt4* mutants at these stages (not shown). Scale bars equal 100 microns.

in Table 1, while *Wnt9b*-expressing NIH3T3 cells failed to induce RV formation within 72 hr, coculture with *Wnt9b*-expressing L cells led to a robust induction of RV formation in isolated MM (26/26, Table 1 and Figure S2A), while L cells alone had no effect (0/22, Table 1 and Figure S2D). The difference between the two cellular sources of Wnt9b is unclear. They may reflect differences in the level of production of active protein, but this cannot be assessed at present. In summary, these data suggest that Wnt9b acts as a direct paracrine factor in the induction of MM.

Table 1. Tubule Induction by Wnt4 and Wnt9b

	# Induced Tubules/Treated Mesenchyme		
Inducer	Wild-Type Mesenchyme	Wnt9b$^{-/-}$ Mesenchyme	Wnt4$^{-/-}$ Mesenchyme
Spinal cord	5/5	NA	NA
NIH3T3-Lac-Z	0/12	0/6	NA
L-Cells	0/22	NA	NA
NIH3T3-Wnt4	11/11	9/10	NA
NIH3T3-Wnt9b	1/31	NA	NA
L-Wnt9b	26/26	NA	0/9

Wild type, Wnt9b$^{-/-}$, or Wnt4$^{-/-}$ mutant mesenchymes were grown in the presence of various inductive tissues or transfected cells. Tubulogenesis was assayed after 72 hr of culturing.

As discussed earlier, Wnt4 acts downstream of Wnt9b, and Wnt4 signaling is both necessary in vivo and sufficient in the MM culture assays described above for induction of RVs in the early kidney. To address the possibility that Wnt9b and Wnt4 bind to the same receptor and activate the same cellular pathway, we tested the ability of *Wnt9b* L cells to induce RV formation in *Wnt4* mutant mesenchyme. No induction was observed, and therefore, Wnt9b cannot functionally substitute for Wnt4 (Table 1 and Figure S2A). In contrast, Wnt4 does not require prior Wnt9b signaling for RV induction (Table 1 and Figure S2B). Taken together, these data suggest that Wnt9b and Wnt4 bind distinct receptors and Wnt4 is itself competent to activate the entire tubulogenic program downstream of Wnt9b.

Mesonephric Tubules and Müllerian Ducts Are Not Induced in *Wnt9b* Mutants

Given the failure of RV induction in the metanephric kidney and the absence of the mesonephric-derived epididymal component of the testes in *Wnt9b*$^{-/-}$ neonates (Figures 2G and 2H), we examined mesonephric tubule

induction. At E11.5, in contrast to *Wnt9b*$^{+/-}$ embryos, no histologically detectable mesonephric tubules were observed in *Wnt9b*$^{-/-}$ embryos (Figures 5A and 5B). In wild-type and *Wnt9b*$^{+/-}$ embryos at E10.5, Pax2 was expressed in the Wolffian duct and induced in adjacent mesonephric tubules and mesenchyme (Figure 5C). However, in *Wnt9b*$^{-/-}$ embryos, Pax2 expression was detected only in the Wolffian duct (Figure 5D). Further, all other mesonephric tubule markers examined (*Lhx1*, *Pax8*, *Fgf8*, and *Wnt4*) were also absent (data not shown). Thus, Wnt9b is essential for both mesonephric and metanephric tubule induction. Interestingly, whereas Wnt4 is downstream of Wnt9b signaling in both of these inductive interactions, in contrast to the metanephric kidney, Wnt4 is not essential for the formation of mesonephric tubules (Stark et al., 1994, and data not shown).

In addition to inducing the mesonephric tubules, the Wolffian duct is also required for Müllerian duct development and consequently development of much of the female reproductive tract (Kobayashi and Behringer, 2003). The anterior-most anlagen of the Müllerian duct forms by an initial invagination of the coelomic epithelium at E11.0–E11.5, generating a coelomic opening, the infundibulum, through which ovulated eggs enter the oviduct. The Müllerian duct then elongates posteriorly to the cloacal region in a Wolffian duct-dependent process that is poorly understood (Gruenwald, 1942). One possible mechanism for posterior growth is the incorporation of intermediate mesoderm by a process of MET (Kobayashi and Behringer, 2003). In wild-type embryos, the Müllerian duct expresses several regulatory factors including *Pax2*, *Lhx1*, *Pax8*, and *Wnt7a* (Figures 5E–5H and not shown). While all of these genes were present in *Wnt9b* mutants, expression was restricted to an anterior epithelial structure that corresponds to the initial coelomic invagination. Thus, while *Wnt9b* is not required for this event, *Wnt9b* is essential for posterior extension of the Müllerian duct and the generation of a functional female reproductive tract.

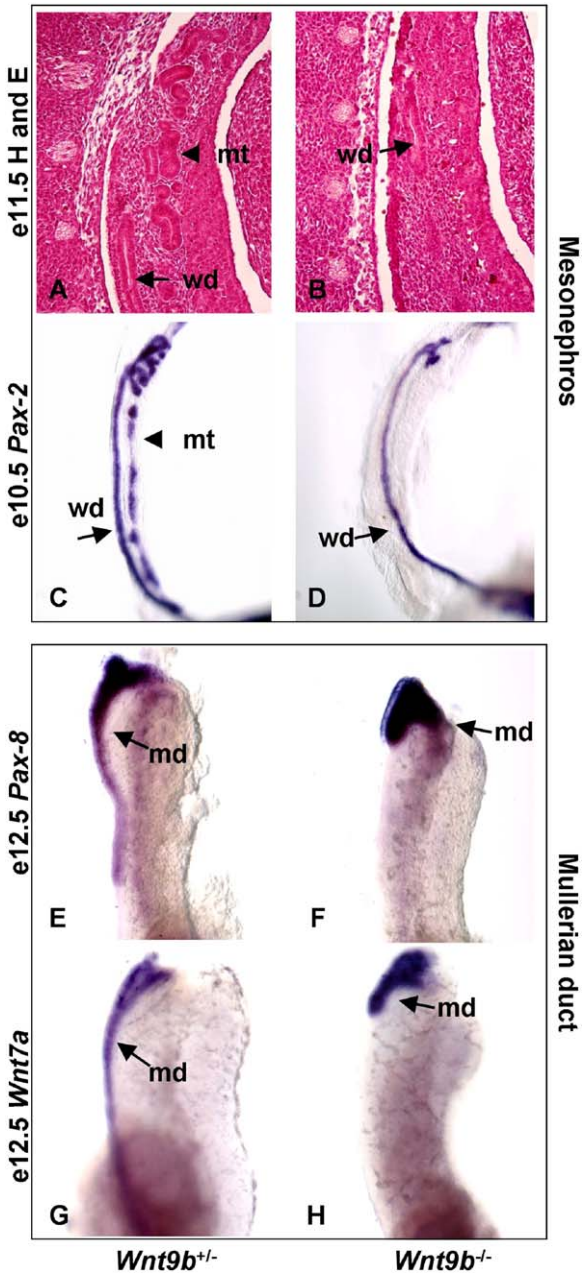

Figure 5. The Mesonephric Tubules and Müllerian Ducts Do Not Form in *Wnt9b* Mutants

A well-formed Wolffian duct (arrow in [A]) and mesonephric tubules (arrowhead in [A]) are visible in hematoxylin and eosin-stained section through a wild-type E11.5 urogenital system. In sections through *Wnt9b* mutants, the Wolffian duct is visible (arrow in [B]), but there is no sign of mesonephric tubules. At E10.5, *Pax2* is expressed in the Wolffian duct (arrow in [C]) and mesonephric tubules (arrowhead in [C]) of wild-type embryos. In *Wnt9b* mutants, expression in the Wolffian duct is maintained (arrow in [D]), but expression in the medial mesenchymal population is not detected. *Pax8* (E and F) and *Wnt7a* (G and H) mark the developing Müllerian duct. In wild-type embryos at E12.5 (E and G), the Müllerian duct (black arrows) forms on the lateral side of the Wolffian duct, extending from the anterior-most portion of the urogenital system toward the bladder. In *Wnt9b* mutants (F and H), only the anterior-most portion of the Müllerian duct forms (black arrows) although the Wolffian duct appears normal (not shown). Identical results were obtained with probes to *Pax-2* and *Lhx1* (not shown).

Canonical Wnt Signaling in Urogenital Development

Several transduction pathways have been proposed to mediate Wnt signaling (Bejsovec, 2005; Chen et al., 2005). The best studied is the canonical pathway, which operates through the stabilization and accumulation of cytoplasmic β-catenin, which then enters the nucleus, where it interacts with the Lef/Tcf family of transcription factors to initiate target gene expression (Giles et al., 2003). Although assignment of specific Wnts to a pathway may be receptor/cell type dependent, several wnts, most notably Wnt1 and Wnt3a, are thought to primarily if not exclusively signal through the canonical pathway. To determine whether a canonical Wnt signal can substitute for Wnt9b, we used a transgenic rescue wherein a Wnt1:GFP fusion protein was activated within the Wolffian duct of *Wnt9b* mutant embryos (Figure 6A). Interestingly, expression of this transgene was sufficient to rescue mesonephric and metanephric tubule induction, as well as caudal extension of the Müllerian duct, in *Wnt9b*$^{-/-}$ mutants (Figures 6B–6D and data not shown). These data implicate a canonical Wnt

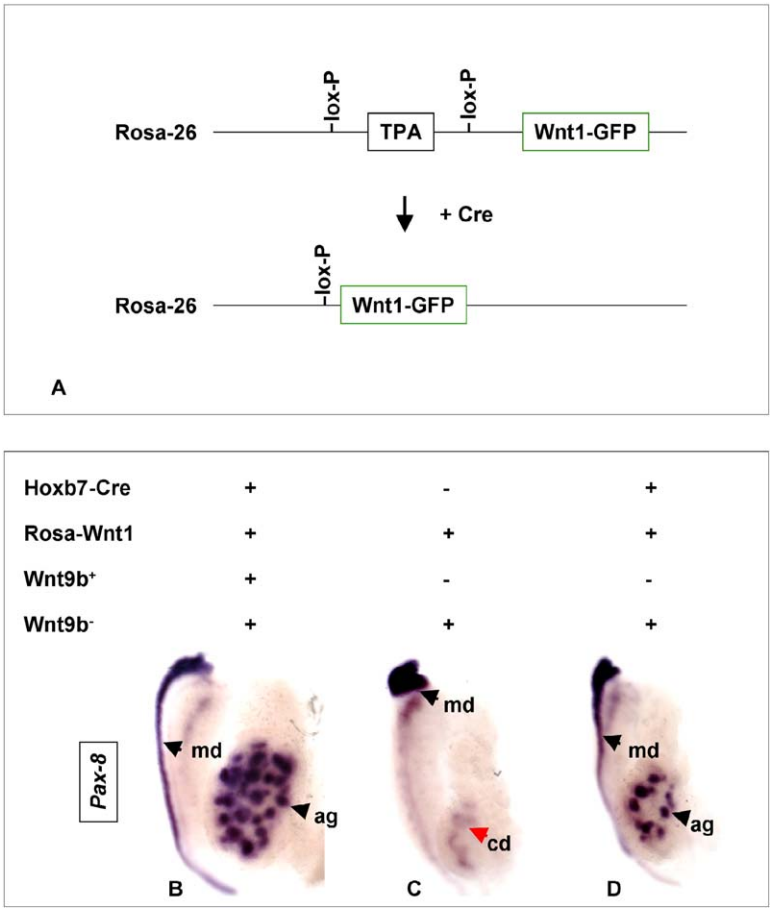

Figure 6. Wnt1-Mediated Rescue of Wolffian Duct Signaling in *Wnt9b* Mutant Embryos

(A) Targeting construct design for ROSA-Wnt1. A full-length Wnt1-GFP fusion construct was inserted into the ubiquitous Rosa-26 locus, downstream of a floxed triple polyadenylation sequence (TPA). Upon exposure to Cre recombinase (in this case a ureteric bud expressed Hoxb7-Cre), the TPA cassette is removed and Wnt1-GFP is expressed.

(B–D) E12.5 urogenital systems from *Hoxb7-Cre; ROSA-Wnt1; Wnt9b* $^{+/-}$ (B), *ROSA-Wnt1; Wnt9b*$^{-/-}$ (C), and *Hoxb7-Cre; ROSA-Wnt1*; *Wnt9b*$^{-/-}$ (D) embryos hybridized with antisense probe for *Pax8*. Ectopic expression of *Wnt1* in the Wolffian duct/ureteric bud has no effects on normal urogenital development (B). Embryos form a normal kidney with normal Wolffian and Müllerian ducts (black arrow). *Wnt9b* null embryos hemizygous for the *ROSA-Wnt1* allele in the absence of a *Hoxb7-Cre* transgene are indistinguishable from *Wnt9b* nulls ([C] and not shown); Müllerian duct development is arrested (black arrow in [C]) and no pretubular aggregates are evident despite invasion of the UB (red arrow in [C]). *Hoxb7-Cre*-driven activation of *ROSA-Wnt1* rescues metanephric tubule induction (black arrowhead in [D]) and Müllerian duct elongation (black arrow) in *Wnt9b* null embryos. ag, pretubular aggregates; cd, ureteric bud-derived collecting duct epithelium; md, Müllerian duct.

signaling process in the development of the urogenital system.

Discussion

Our data indicate that Wnt9b acts as a general organizing signal in the Wolffian duct-dependent elaboration of several distinct components of the mouse urogenital system. Although the inducing capabilities of the Wolffian duct and its derivative, the ureteric bud, have been known for over 50 years (Grobstein, 1953, 1955), the molecular nature of the relevant signals has remained elusive.

The data herein argue for a continuum of Wnt signaling in the normal process of RV induction. First, *Wnt9b* appears to act as a paracrine signal, from ureteric bud to metanephric mesenchyme, to initiate a tubulogenic program through the activation of *Pax8*, *Fgf8*, and *Wnt4* in the pretubular MM. Several findings argue against an alternative conclusion, that the failure of MM induction is an indirect outcome of altered growth or survival of the inducing (UB) or responding (MM) tissue. First, we fail to observe a decrease in cell growth coincident with the initial inductive stages at E11.5. Second, UB growth, primary branching, and patterning is unaltered in *Wnt9b* mutants. Third, although at E11.5 the mutant MM does not express any pretubular markers, it is of a normal size and expresses normal levels of a number of markers associated with the uninduced MM progenitor state (e.g., *Pax2, Eya1, WT1*, and *Six2*). Fourth, the MM is normally positioned as a tight cap around the branched UB in *Wnt9b* mutants, arguing against a physical disruption of a short-range signaling process.

Wnt9b-dependent activation of *Wnt4* expression in the MM itself plays a central role in completing the process of tubule induction. Like Wnt9b, Wnt4 is essential for early RV induction (Stark et al., 1994). However, the analysis of *Wnt9b* and *Wnt4* mutants suggests Wnt9b-dependent and Wnt4-independent regulation of a primary inductive response (e.g., activation of *Wnt4*, *Pax8*, and *Fgf8*). Despite these differences, Wnt4-producing fibroblasts can rescue *Wnt9b* deficiency, suggesting that activation of *Wnt4* is the key downstream step in the mesenchymal response to inductive signaling. One striking difference between the two genetic models is the cessation of UB branching at the T-stage of *Wnt9b* mutants and a relatively normal pattern of branching in *Wnt4* mutants up until E13.5 despite a complete absence of initial RV induction in both models. Decreased expression of *GDNF* in the MM, a factor previously shown to be essential for normal branching morphogenesis (Angrist et al., 1996; Durbec et al., 1996; Moore et al., 1996; Pichel et al., 1996), most likely explains the more extreme *Wnt9b*$^{-/-}$ branching phenotype. The differences observed in the two Wnt mutants presuma-

bly reflect either the activation of Wnt9b-dependent, Wnt4-independent factors within the mesenchyme or additional roles for Wnt9b signaling within the ureteric epithelium. At present we cannot distinguish between these alternative explanations.

Although the Wolffian duct and UB are necessary for the formation of the mesonephric and metanephric tubules, respectively, it has been suggested that disparate molecular mechanisms are utilized in these events (Gruenwald, 1952; Saxen, 1987). Our findings indicate that Wnt9b provides a common molecular link between these inductive processes, as well as in the caudal extension of the Müllerian duct. It is tempting to speculate that induction of a MET may represent a common cellular program. MET is clearly shared between the mesonephric and metanephric tubules, and although the cellular processes regulating the posterior growth of the Müllerian duct are unknown, they may involve the incorporation of cells from the intermediate mesoderm into a migrating epithelium, as suggested for Wolffian duct development (Cornish and Etkin, 1993; Drawbridge et al., 2003).

These results raise the question of the signaling pathways that underpin Wnt9b and Wnt4 action in their target tissues. The simplest hypothesis, that these inductive ligands activate a common receptor pathway, is not supported by the finding that Wnt9b-expressing cells fail to rescue Wnt4 mutant mesenchyme, whereas the same cells are able to induce RV formation in wild-type MM explants. Thus, Wnt9b and Wnt4 may act through distinct receptors. Several members of the Frizzled family of Wnt receptors are expressed in the MM at the relevant stages, but genetic and biochemical analyses of their potential roles in mediating Wnt signaling await further study. Interestingly, a canonical Wnt signal, Wnt1, can rescue all aspects of *Wnt9b* deficiency, implicating a canonical Wnt pathway downstream of receptor activation (Plisov et al., 2001). Both Wnt9b and Wnt4 can stabilize β-catenin in responsive tissue culture cells; however, both signals have much weaker activity in these assays than well-studied canonical Wnt ligands (data not shown).

In summary, our data suggest that the general organizing properties of the Wolffian duct and its derivatives are mediated by a common signal, Wnt9b. Although a MET may represent a common cellular output, the resulting tubular structures formed by adjacent cell populations are distinct. These findings suggest that Wnt9b encodes a permissive signal, the region-specific response being governed by either the interplay of additional signaling factors or preprogramming of the target cell response by early patterning processes.

Experimental Procedures

In Situ Hybridization

In situ hybridization was performed on whole embryos (E9.5–E12.5) and dissected urogenital systems (E11.5–E18.5) obtained from timed pregnancies utilizing the Holle Huttner liquid handling system. Noon of the day of plugging was considered 12 hr postcoitum or E0.5. Tissues were fixed in 4% paraformaldehyde (PFA) at 4°C overnight. For mutant analysis, a minimum of five heterozygous and five homozygous embryos were analyzed. Hybridized embryos were cleared in 80% glycerol and photographed using a Nikon digital still camera (DXM1200) on a Nikon stereomicroscope (SMZ1500).

Immunohistochemistry

E11.5, E13.5, and E15.5 embryos were fixed in 4% paraformaldehyde at 4°C overnight then imbedded in paraffin wax. Dewaxed sections were incubated with primary antibodies to Pax2 (Covance), pan-cytokeratin (Sigma), E-cadherin (Zymed), Laminin (Sigma), and DBA lectin (Sigma) and the secondary antibodies Alexa 488 and 568 (Molecular Probes). Sections were viewed and photographed on a Zeiss LSM510 Axioplan inverted confocal microscope.

Library Screening and 5′RACE

A ^{32}P-labeled probe was synthesized from a gel-purified, 350 base pair *Wnt9b* cDNA fragment (Bergstein et al., 1997). The probe was hybridized to a gridded, E18.5 kidney cDNA library. Out of 96,000 individual clones screened, only one *Wnt9b* cDNA was identified (referred to as *kWnt9b-1*). Restriction mapping and sequence analysis revealed that this clone contained an open reading frame that was homologous to approximately the last 250 amino acids of several Wnts and a long (3800 base pair), polyadenylated, 3′ untranslated region, but lacked a probable 5′ start AUG and signal peptide.

In order to identify the start AUG, we performed 5′RACE on single-stranded cDNA generated from E12.5 kidney RNA utilizing a primer (5′-cccgtttcgcgagaccggcca-3′) at the 5′ end of the partial *Wnt9b* cDNA sequence. Initially this strategy identified an additional 249 base pairs of 5′ sequence that still lacked an initiation codon. An additional round of 5′ RACE was performed using a more 5′ primer 5′-gcctgaccggtcgtgaggtcc-3′ that extended another 65 base pairs. This product contained an in-frame ATG. RT-PCR was performed on E12.5 cDNA with primers to the predicted 5′ UTR and ATG (5′-ggcagacagagctgctATGGCAT-3′) and the translation termination TAG (5′-CTAGcgcttgcaggtatacacgagctc-3′) utilizing high-fidelity pfu polymerase. A single band of the predicted size (1042 base pairs) was amplified, cloned into pZero (Invitrogen), and sequenced, confirming that the predicted *Wnt9b* open reading frame is encoded in a contiguous mRNA in the embryonic kidney. In order to identify whether this mRNA contained a consensus signal peptide, the sequence downstream of the potential AUG was analyzed with the SIGFIND software (http://139.91.72.10/sigfind/sigfind.html). Three of four algorithms run predicted that the protein coded for by this cDNA was not a secreted molecule, although a FLAG-tagged version of this protein can be found within the Golgi apparatus and endoplasmic reticulum in transfected cells (not shown). Other clones containing an alternative ATG have been identified (Qian et al., 2003), and therefore we suggest calling this isoform *Wnt9b.2* and the alternative isoform *Wnt9b.1*. Because *Wnt9b.1* contains a consensus signal peptide, it was used for all further in vitro experimentation.

Generation of Wnt9b Conditional Null ES Cell Lines

The genomic structure of *Wnt9b* was determined utilizing both the Celera and publicly available sequence of the mouse genome and a targeting vector designed (Figure S1). The original 300 base pair cDNA fragment was used to probe a 129/Svj Bac genomic DNA library (Genome Systems). This Bac was used as a template for the generation of a conditionally inactive allele by amplifying a region of DNA flanking exon 2 (p3, 5′-atgcatggtctgtaaccaatccttgc-3′; p4, 5′-ggccggccgatgagcgtgtggacaaagg-3′) and two additional arms of homology 5′ (p1, 5′-atcgatcggaagtgttccctacactc-3′; p2, 5′-ggcgcgccggtaggacacactccagagt-3′) and 3′ (p5, 5′-gcggccgcctgtcactgttcgtcacatc-3′; p6, 5′-ggcgcgccctctccacctctgggctgtg-3′) to exon 2, utilizing a cocktail of high-fidelity Pfu polymerase and Taq polymerase. Enzyme sites were added to the 5′ end of all oligos to aid in subcloning. All three subclones were sequenced completely to verify that no mutations were introduced in the PCR. The three subclones were cloned into a neomycin/thymidine kinase double selection vector. The exon 2-containing subclone was ligated into a multiple cloning site flanked by loxp sites. Flp recombinase target (frt) sites flanked the neomycin resistance cassette. This construct was electroporated into the AV3 embryonic stem cell line. 5′ and 3′ external probes were PCR amplified and cloned into the pZero vector (Invitrogen). Primers for the 5′ probe were p7, 5′-ctgctg tggccactgtccca-3′, and p8, 5′-gtcctggtcccagcatctcc-3′; for the 3′

probe, they were p9, 5′-gggccacacgtctgcttcca-3′, and p10, 5′-ccaggatgcaatgggactct-3′ (Figure S1). Purified genomic DNA from individual clones was digested with EcoRI and screened by Southern blot for homologous recombination using both external probes to identify a correctly targeted ES clone (1 in 596; Figure S1). This clone was injected into C57BL6/J blastocysts and a *Wnt9b*-targeted mouse line established from germline-transmitting chimeras (see text).

Litters were genotyped by PCR utilizing a cocktail of three primers: p11, 5′-gcagaatctggagaacttggc-3′; p12, 5′-gtgagaaggaagatggtgagc-3′; and p13, 5′-tctccaggtatggtggatgg-3′ (93°C, 2 min; 93°C, 30 s; 58°C, 30 s; 72°C, 1 min; 35 times to step two). The wild-type allele (p11 + p12) gives a band of 250 base pairs while the null allele (p11 + p13) gives a band of 500 base pairs (Figure S1).

NIH/3T3 Metanephric Mesenchyme Coculture

Metanephric mesenchyme was separated from E11–E11.5 wild-type or Wnt9b$^{-/-}$ ureteric buds as previously described (Sainio, 2003b). Mesenchymes were cocultured with dorsal spinal cord or cells expressing the *E. coli Lac-Z, Wnt1, Wnt3a, Wnt4,* or *Wnt9b-1*. To generate Wnt9b-expressing cell lines, a full-length Wnt9b cDNA was cloned into pIRES2-EGFP or pGKS2P+ vector and transfected into NIH3T3 or L-cells, respectively. Stable lines were selected by growing transfectants in 1 or 0.4 mg/ml G418 for 3 weeks. Several individual clones for both cell types were tested for their ability to induce tubulogenesis. A third line was created by infecting NIH3T3 cells with a retrovirus containing a full-length *Wnt9b.1* cDNA. This construct has previously been shown to be active in vitro (Qian et al., 2003).

Generation of Rosa26 Wnt1EGFP Mice

To generate a Wnt1EGFP fusion construct, a blunt-ended, Nco I fragment containing the entire *Wnt1* coding region was subcloned into a blunt-ended, BamHI-digested mEGFP construct (Okada et al., 1999). In order to test this construct for activity, it was subcloned into the CS2+ and pCIG plasmids for misexpression analysis in *Xenopus* embryos and chicken neural tube, respectively. Activity of the tagged construct was similar to an untagged version (not shown).

The Wnt1EGFP fragment was isolated by Kpn I digestion, end-filled, Not I-digested, and subcloned into BigT vector (Srinivas et al., 2001) using the Not I and Sal I (blunted) sites to generate BigWnt1EGFP. A Pac I/Asc I fragment of BigWnt1EGFP was cloned into Pac I, Asc I-digested Rosa26PA (Srinivas et al., 2001) to generate Rosa26Wnt1EGFP.

40 μg of Rosa26Wnt1EGFP DNA was electroporated into mouse AV3 embryonic stem cells. Homologous recombinants were identified by Southern blotting following EcoR V digestion of genomic DNA from each clone as previously described (Srinivas et al., 2001). Blastocyst injection of the Rosa26Wnt1EGFP ES cells was carried out as previously described. To drive expression in the Wolffian duct and ureteric bud, mice carrying the transgene were crossed with mice containing a Hoxb7-Cre transgene (Yu et al., 2002).

Supplemental Data

Supplemental Data include two figures and can be found with this article online at http://www.developmentalcell.com/cgi/content/full/9/2/283/DC1/.

Acknowledgments

The authors would like to thank Diane Faria, Joe Vaughan, Big John Bett, Mary Duah, and Jill McMahon for their technical support, Anthony Brown for providing the Wnt15 cDNA fragment, Greg Shackleford for providing Wnt9b-infected cells, and Louis Reichhardt for providing in situ probes. A.P.M. was supported by a grant from the National Institutes of Health, and T.J.C. was supported by the American Cancer Society and the Polycystic Kidney Research Foundation.

Received: August 18, 2004
Revised: April 8, 2005
Accepted: May 19, 2005
Published: August 1, 2005

References

Angrist, M., Bolk, S., Halushka, M., Lapchak, P.A., and Chakravarti, A. (1996). Germline mutations in glial cell line-derived neurotrophic factor (GDNF) and RET in a Hirschsprung disease patient. Nat. Genet. *14*, 341–344.

Barasch, J., Yang, J., Ware, C.B., Taga, T., Yoshida, K., Erdjument-Bromage, H., Tempst, P., Parravicini, E., Malach, S., Aranoff, T., and Oliver, J.A. (1999). Mesenchymal to epithelial conversion in rat metanephros is induced by LIF. Cell *99*, 377–386.

Bard, J.B., Gordon, A., Sharp, L., and Sellers, W.I. (2001). Early nephron formation in the developing mouse kidney. J. Anat. *199*, 385–392.

Bejsovec, A. (2005). Wnt pathway activation: new relations and locations. Cell *120*, 11–14.

Bergstein, I., Eisenberg, L.M., Bhalerao, J., Jenkins, N.A., Copeland, N.G., Osborne, M.P., Bowcock, A.M., and Brown, A.M. (1997). Isolation of two novel WNT genes, WNT14 and WNT15, one of which (WNT15) is closely linked to WNT3 on human chromosome 17q21. Genomics *46*, 450–458.

Boyden, E.A. (1927). Experimental obstruction of the mesonephric ducts. Proc. Soc. Exp. Biol. Med. *25*, 572–576.

Carroll, T.J., and McMahon, A.P. (2003). Overview: the molecular basis of kidney development. In The Kidney: From Normal Development to Congenital Disease, Peter D. Vize and Johnathan B.L. Bard, eds. (Boston: Academic Press), pp. 343–376.

Chen, A.E., Ginty, D.D., and Fan, C.M. (2005). Protein kinase A signalling via CREB controls myogenesis induced by Wnt proteins. Nature *433*, 317–322.

Cornish, J.A., and Etkin, L.D. (1993). The formation of the pronephric duct in *Xenopus* involves recruitment of posterior cells by migrating pronephric duct cells. Dev. Biol. *159*, 338–345.

Donovan, M.J., Natoli, T.A., Sainio, K., Amstutz, A., Jaenisch, R., Sariola, H., and Kreidberg, J.A. (1999). Initial differentiation of the metanephric mesenchyme is independent of WT1 and the ureteric bud. Dev. Genet. *24*, 252–262.

Drawbridge, J., Meighan, C.M., Lumpkins, R., and Kite, M.E. (2003). Pronephric duct extension in amphibian embryos: migration and other mechanisms. Dev. Dyn. *226*, 1–11.

Durbec, P., Marcos-Gutierrez, C.V., Kilkenny, C., Grigoriou, M., Wartiowaara, K., Suvanto, P., Smith, D., Ponder, B., Costantini, F., Saarma, M., et al. (1996). GDNF signalling through the Ret receptor tyrosine kinase. Nature *381*, 789–793.

Giles, R.H., van Es, J.H., and Clevers, H. (2003). Caught up in a Wnt storm: Wnt signaling in cancer. Biochim. Biophys. Acta *1653*, 1–24.

Godin, R.E., Takaesu, N.T., Robertson, E.J., and Dudley, A.T. (1998). Regulation of BMP7 expression during kidney development. Development *125*, 3473–3482.

Grobstein, C. (1953). Inductive epithlio-mesenchymal interaction in cultured organ rudiments of the mouse metanephros. Science *118*, 52–55.

Grobstein, C. (1955). Inductive interaction in the development of the mouse metanephros. J. Exp. Zool. *130*, 319–340.

Gruenwald, P. (1937). Zur Entwicklungmechanik der Urogenital-systems beim Huhn. Wilhelm Roux Arch Entw Mech *136*, 786–813.

Gruenwald, P. (1942). Common traits in development and stucture of the organs originating from the coelomic wall. J. Morphol. *70*, 353–387.

Gruenwald, P. (1952). Development of the excretory system. Ann. N Y Acad. Sci. *55*, 142–146.

Herzlinger, D., Qiao, J., Cohen, D., Ramakrishna, N., and Brown, A.M. (1994). Induction of kidney epithelial morphogenesis by cells expressing Wnt-1. Dev. Biol. *166*, 815–818.

Jing, S., Wen, D., Yu, Y., Holst, P.L., Luo, Y., Fang, M., Tamir, R.,

Antonio, L., Hu, Z., Cupples, R., et al. (1996). GDNF-induced activation of the ret protein tyrosine kinase is mediated by GDNFR-alpha, a novel receptor for GDNF. Cell *85*, 1113–1124.

Kalatzis, V., Sahly, I., El-Amraoui, A., and Petit, C. (1998). Eya1 expression in the developing ear and kidney: towards the understanding of the pathogenesis of Branchio-Oto-Renal (BOR) syndrome. Dev. Dyn. *213*, 486–499.

Kirikoshi, H., Sekihara, H., and Katoh, M. (2001). Molecular cloning and characterization of WNT14B, a novel member of the WNT gene family. Int. J. Oncol. *19*, 947–952.

Kispert, A., Vainio, S., and McMahon, A.P. (1998). Wnt-4 is a mesenchymal signal for epithelial transformation of metanephric mesenchyme in the developing kidney. Development *125*, 4225–4234.

Kobayashi, A., and Behringer, R.R. (2003). Developmental genetics of the female reproductive tract in mammals. Nat. Rev. Genet. *4*, 969–980.

Majumdar, A., Vainio, S., Kispert, A., McMahon, J., and McMahon, A.P. (2003). Wnt11 and Ret/Gdnf pathways cooperate in regulating ureteric branching during metanephric kidney development. Development *130*, 3175–3185.

Moore, M.W., Klein, R.D., Farinas, I., Sauer, H., Armanini, M., Phillips, H., Reichardt, L.F., Ryan, A.M., Carver-Moore, K., and Rosenthal, A. (1996). Renal and neuronal abnormalities in mice lacking GDNF. Nature *382*, 76–79.

Mori, K., Yang, J., and Barasch, J. (2003). Ureteric bud controls multiple steps in the conversion of mesenchyme to epithelia. Semin. Cell Dev. Biol. *14*, 209–216.

Muller, U., Wang, D., Denda, S., Meneses, J.J., Pedersen, R.A., and Reichardt, L.F. (1997). Integrin alpha8beta1 is critically important for epithelial-mesenchymal interactions during kidney morphogenesis. Cell *88*, 603–613.

Okada, A., Lansford, R., Weimann, J.M., Fraser, S.E., and McConnell, S.K. (1999). Imaging cells in the developing nervous system with retrovirus expressing modified green fluorescent protein. Exp. Neurol. *156*, 394–406.

Pichel, J.G., Shen, L., Sheng, H.Z., Granholm, A.C., Drago, J., Grinberg, A., Lee, E.J., Huang, S.P., Saarma, M., Hoffer, B.J., et al. (1996). Defects in enteric innervation and kidney development in mice lacking GDNF. Nature *382*, 73–76.

Plisov, S.Y., Yoshino, K., Dove, L.F., Higinbotham, K.G., Rubin, J.S., and Perantoni, A.O. (2001). TGF beta *2*, LIF and FGF2 cooperate to induce nephrogenesis. Development *128*, 1045–1057.

Qian, J., Jiang, Z., Li, M., Heaphy, P., Liu, Y.H., and Shackleford, G.M. (2003). Mouse Wnt9b transforming activity, tissue-specific expression, and evolution. Genomics *81*, 34–46.

Sainio, K. (2003a). Development of the mesonephric kidney. In The Kidney: From Normal Development to Congenital Disease, Peter D. Vize and Johnathan B.L. Bard, eds. (Boston: Academic Press), pp. 75–86.

Sainio, K. (2003b). Experimental methods for studying urogenital development. In The Kidney: From Normal Development to Congenital Disease, Peter D. Vize and Johnathan B.L. Bard, eds. (Boston: Academic Press), pp. 327–343.

Sanchez, M.P., Silos-Santiago, I., Frisen, J., He, B., Lira, S.A., and Barbacid, M. (1996). Renal agenesis and the absence of enteric neurons in mice lacking GDNF. Nature *382*, 70–73.

Saxen, L. (1987). Organogenesis of the Kidney (New York: Cambridge University Press).

Schuchardt, A., D'Agati, V., Larsson-Blomberg, L., Costantini, F., and Pachnis, V. (1994). Defects in the kidney and enteric nervous system of mice lacking the tyrosine kinase receptor Ret. Nature *367*, 380–383.

Schuchardt, A., D'Agati, V., Pachnis, V., and Costantini, F. (1996). Renal agenesis and hypodysplasia in ret-k^{-} mutant mice result from defects in ureteric bud development. Development *122*, 1919–1929.

Srinivas, S., Watanabe, T., Lin, C.S., William, C.M., Tanabe, Y., Jessell, T.M., and Costantini, F. (2001). Cre reporter strains produced by targeted insertion of EYFP and ECFP into the ROSA26 locus. BMC Dev. Biol. *1*, 4.

Stark, K., Vainio, S., Vassileva, G., and McMahon, A.P. (1994). Epithelial transformation of metanephric mesenchyme in the developing kidney regulated by Wnt-4. Nature *372*, 679–683.

Tomac, A.C., Grinberg, A., Huang, S.P., Nosrat, C., Wang, Y., Borlongan, C., Lin, S.Z., Chiang, Y.H., Olson, L., Westphal, H., and Hoffer, B.J. (2000). Glial cell line-derived neurotrophic factor receptor alpha1 availability regulates glial cell line-derived neurotrophic factor signaling: evidence from mice carrying one or two mutated alleles. Neuroscience *95*, 1011–1023.

Treanor, J.J., Goodman, L., de Sauvage, F., Stone, D.M., Poulsen, K.T., Beck, C.D., Gray, C., Armanini, M.P., Pollock, R.A., Hefti, F., et al. (1996). Characterization of a multicomponent receptor for GDNF. Nature *382*, 80–83.

Waddington, C.H. (1938). The morphogenetic functions of vestigial organs in the chick. J. Exp. Biol. *15*, 371–376.

Yu, J., Carroll, T.J., and McMahon, A.P. (2002). Sonic hedgehog regulates proliferation and differentiation of mesenchymal cells in the mouse metanephric kidney. Development *129*, 5301–5312.